Lawrence Berkeley National Laboratory

Lawrence Berkeley National Laboratory

Title
Electron-cloud Build-up Simulations in the Proposed PS2: Status Report

Permalink
https://escholarship.org/uc/item/0dj5c3c4

Author
Furman, M. A.

Publication Date
2010-06-30

ELECTRON-CLOUD BUILD-UP SIMULATIONS IN THE PROPOSED PS2: STATUS REPORT[*]

M. A. Furman,[†] LBNL, Berkeley, CA, USA

R. De Maria, Y. Papaphilippou, G. Rumolo, CERN, Geneva, Switzerland

Abstract

A replacement for the PS storage ring is being considered, in the context of the future LHC accelerator complex upgrade, that would likely place the new machine (the PS2) in a regime where the electron-cloud (EC) effect might be significant. We report here our current estimate of the EC density n_e in the bending magnets and the field-free regions at injection and extraction beam energy, for both proposed bunch spacings, $t_b = 25$ and 50 ns. The primary model parameters exercised are the peak secondary emission yield (SEY) $\delta_{\max}$, the electron-wall impact energy at which the SEY peaks, $E_{\max}$, and the chamber radius a in the field-free regions. We present many of our results as a function of the bunch intensity N_b, and we provide a tentative explanation for the non-monotonic behavior of n_e as a function of N_b.

INTRODUCTION

In the results presented here we employed the EC build-up simulation codes ECLOUD [1] and POSINST [2], which have been well benchmarked against each other [3]. In each case analyzed, we estimated the electron-cloud density by time-averaging over two beam batches. For the 25-ns spacing option, a batch is defined as a train of 168 full consecutive buckets followed by 12 empty buckets. For the 50-ns spacing option, a batch is defined by a sequence of 84 bunches filling every other bucket, followed by 12 empty buckets. Other parameters are summarized in Table 1. For the sake of simplicity at this stage of the simulation process, we assumed the same bunch sizes in the field-free region and in the dipole bending magnet.

DEPENDENCE ON $\delta_{\max}$

The primary variable that determines the build-up of n_e is $\delta_{\max}$. We have assumed a model for the secondary electron emission spectrum that approximately represents stainless steel [2]. By varying $\delta_{\max}$, we conclude that there is a rather clear threshold for significant EC density n_e when $\delta_{\max}$ exceeds ~ 1.3 for the 50 ns option, as seen in Figs. 1 (here n_e represents the temporal and spatial average of the electron density in the section being simulated). For the 25 ns option, threshold is lower, $\delta_{\max} \sim 1.2$.

Table 1: Selected PS2 Parameters used in Simulations.

Ring and beam	
Ring circumference	$C = 1346.4$ m
RF frequency	$f_{\mathrm{RF}} = 40$ MHz
Harmonic number	$h = 180$
Bunch spacing	$t_b = 25$ or 50 ns
Bunch intensity (nom.)	
at $t_b = 25$ ns	4.2×10^{11}
at $t_b = 50$ ns	5.9×10^{11}
Inj./extr. beam kinetic energy	4/50 GeV
Transv. RMS bunch sizes	
at inj.	$(\sigma_x, \sigma_y) = (6.3, 5.9)$ mm
at extr..	$(\sigma_x, \sigma_y) = (1.95, 1.83)$ mm
RMS bunch length at inj./extr.	$\sigma_z = 1.0/0.33$ m
Pipe cross section	
dipole	elliptical, $(a, b) = (6, 3.5)$ cm
field-free	round, $a = 4 - 6$ cm
Dipole bending field at extr.	$B = 1.7$ T
Secondary e⁻ parameters	
Peak SEY	$\delta_{\max} = 1.0 - 1.8$
Electron energy at $\delta_{\max}$	$E_{\max} = 292.6$ eV
SEY at 0 energy	$\delta(0) = 0.2438 \times \delta_{\max}$
Simulation parameters	
Bunch profile	3D gaussian
Full bunch length	$L_b = 5\sigma_z$
Max. no. of macroelectrons	20000
Integration time step	3×10^{-11} s
Space-charge grid size	64×64

DEPENDENCE ON N_b

The dependence of n_e on N_b is shown in Figs. 2. One sees a non-monotonic dependence on N_b, particularly at extraction energy, by virtue of which n_e peaks at a value of N_b that is significantly lower than nominal. For the bending magnets at extraction energy, the explanation of this non-monotonic dependence is almost certainly the following: As N_b increases from low values, the average electron-wall impact energy $\langle E_0 \rangle$ rises roughly proportionally to N_b and crosses the value $E_{\max} \simeq 300$ eV, at which point the SEY is highest, when $N_b \simeq (1 - 3) \times 10^{11}$. As N_b increases beyond this value, $\langle E_0 \rangle$ exceeds $E_{\max}$, hence the effective SEY decreases, hence so does n_e. This non-monotonicity is particularly clear at extraction energy because σ_z is short enough that the beam impulsively imparts energy to the electrons. At injection energy, σ_z is large enough that the beam-electron force is not impulsive due to the phase averaging of the electrons temporarily trapped by the beam
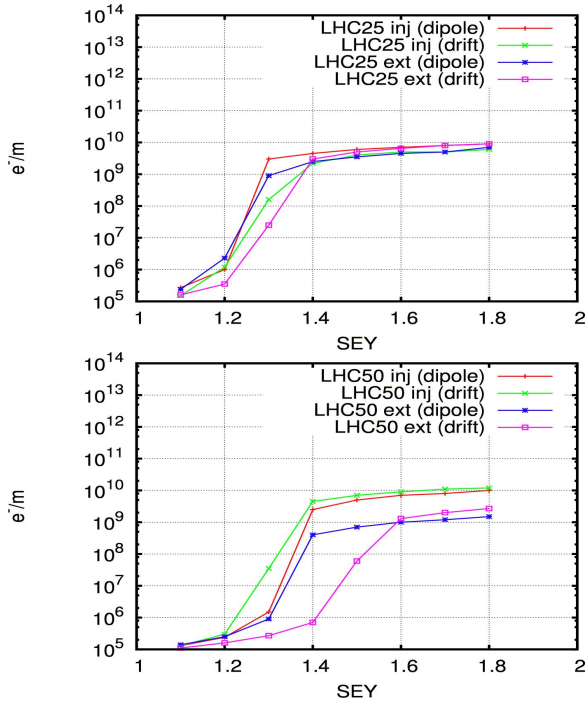
Figure 1: Average EC line density vs. δ_{max}, assuming nominal values for N_b, for $t_b = 25$ (top) and 50 ns (bottom). The line density is proportional to n_e, with 10^{10} e$^-$/m corresponding to $n_e = 1.55 \times 10^{12}$ m^{-3}.

Figure 2: Simulated n_e vs. N_b, assuming $\delta_{\mathrm{max}} = 1.3$. The arrows indicate the nominal design values of N_b for 25 ns (red) and 50 ns (blue) bunch spacing.

potential, hence the proportionality $\langle E_0 \rangle \propto N_b$ is spoiled, hence $\langle E_0 \rangle$ remains below E_{max} up to significantly higher values of N_b. This explanation is probably valid for field-free regions as well (see the discussion below).

SUMMARY OF PRESENT RESULTS

Average EC density

Table 2 summarizes our estimates of the ecloud density for most cases explored, assuming $\delta_{\mathrm{max}} = 1.3$, a value that is generally believed to correspond to conditioned stainless steel, and assuming that the vacuum chamber in the field-free region has a radius $a = 6$ cm. Roughly speaking, the average n_e is in the range (a few)$\times 10^{10}$–(a few)$\times 10^{12}$ m^{-3}, while the local density within the 1σ beam ellipse is in the range (a few)$\times 10^{11}$–(a few)$\times 10^{12}$ m^{-3}. In general, the 50-ns option is clearly favored over the 25-ns option: roughly speaking, the former leads to lower values of n_e by factors of ~ 3 relative to the latter.

Dependence on chamber radius in drift regions

We examined the dependence of n_e on the pipe radius a in the range $a = 4 - 6$ cm. Results at extraction energy are shown in Fig. 3. We conclude that the dependence is weak at nominal values of N_b, but may be significant at lower bunch intensities. For the 50-ns option, however, the results unambiguosly favor a lower value of a. The no-
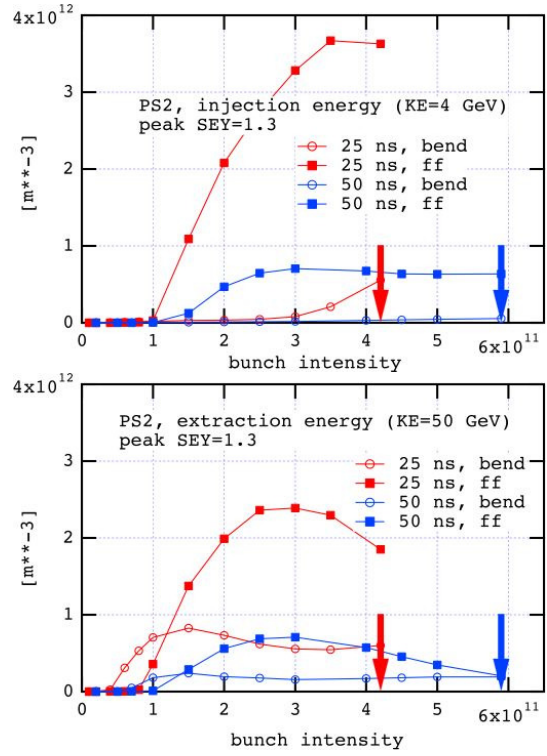
ticeable non-monotonicity of $n_e(a)$ is related to the above-mentioned non-monotonicity of $n_e(N_b)$.

DISCUSSION

We explored the numerical stability of our results against basic computational parameters. We conclude that the value of the integration time step size $\Delta t = 3 \times 10^{-11}$ s is sufficiently small for stable results (the results become unstable when Δt is somewhere in the range $(10 - 50) \times 10^{-11}$ s). Spot-checks showed that space-charge grid sizes 16×16, 32×32 and 64×64 did not yield significant differences; we intend to revisit this somewhat puzzling result.

All results above are for a tri-gaussian bunch profile. We spot-checked the sensitivity of n_e against the transverse and longitudinal bunch profile by considering parabolic transverse bunch shape and flat longitudinal profile. The conclusion is that these bunch shapes lead to slightly lower ($\sim 5 - 10\%$) values of n_e compared with the gaussian shape, in all cases considered.

In order to check the above-mentioned explanation for the non-monotonicity of $n_e(N_b)$, we varied E_{max} while holding all other variables fixed. Results are shown in Fig. 4. As expected, the peak of $n_e(N_b)$ shifts monotonically with N_b. More detailed analysis (not shown here) also show that $\langle E_0 \rangle$ is a fairly linear function of N_b, and furthermore that the value of N_b where n_e peaks is a linear function of the value of N_b at which $\langle E_0 \rangle = E_{\mathrm{max}}$.

Table 2: Estimated n_e (in m^{-3}), Assuming $\delta_{\max} = 1.3$.

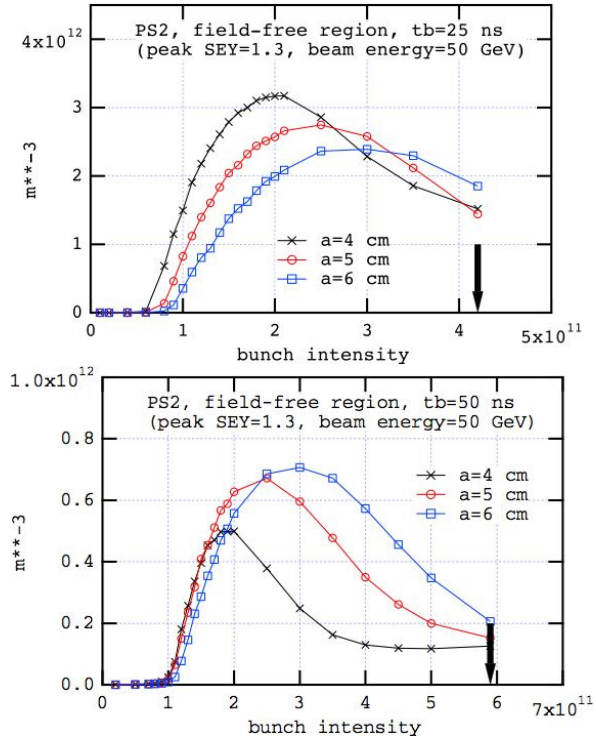|	Injection energy		Extraction energy	
	Bending magnet	Field free region	Bending magnet	Field free region
Overall:				
$t_b = 25$ ns, $N_b = 4.2 \times 10^{11}$	$\sim 6 \times 10^{11}$	$\sim 4 \times 10^{12}$	$\sim 6 \times 10^{11}$	$\sim 2 \times 10^{12}$
$t_b = 50$ ns, $N_b = 5.9 \times 10^{11}$	$\sim 5 \times 10^{10}$	$\sim 6 \times 10^{10}$	$\sim 2 \times 10^{11}$	$\sim 2 \times 10^{11}$
Within the 1σ beam ellipse:				
$t_b = 25$ ns, $N_b = 4.2 \times 10^{11}$	$\sim 5 \times 10^{12}$	$\sim 8 \times 10^{12}$	$\sim 5 \times 10^{12}$	$\sim 6 \times 10^{12}$
$t_b = 50$ ns, $N_b = 5.9 \times 10^{11}$	$\sim 5 \times 10^{11}$	$\sim 2 \times 10^{12}$	$\sim 3 \times 10^{12}$	$\sim 6 \times 10^{11}$

Figure 3: Average n_e vs. N_b in a field-free region at extraction energy, assuming $\delta_{\max} = 1.3$, for 3 values of the chamber radius a.

Figure 4: Average n_e vs. N_b in a dipole bending magnet at extraction energy for various values of $E_{\max}$, assuming $\delta_{\max} = 1.3$ and $t_b = 25$ ns in all cases.

values of n_e than a low-rediffused-component spectrum.

Simulations of the effect of the EC on the beam show a threshold value $n_e \sim 0.5 \times 10^{12}$ m^{-3} for significant instability and/or emittance growth [5]. This value lies in the mid-range of our estimates for n_e. Therefore, while more detailed investigations remain to be carried out, we feel confident to conclude that smooth, reliable, operation of the PS2 will almost certainly require mitigation of the EC, likely via low-emission coatings.

ACKNOWLEDGMENTS

REFERENCES

[1] G. Rumolo and F. Zimmermann, CERN-SL-Note-2002-016-AP.

[2] M. A. Furman and G. R. Lambertson, KEK Proc. 97-17; M. A. Furman and M. T. F. Pivi, PRSTAB **5**, e124404 (2003).

[3] F. Zimmermann et. al., Proc. EPAC04, paper THPLT017.

[4] G. Rumolo, SPS Upgrade Study Team Mtg., Nov. 20, 2007, https:// paf-spsu.web.cern.ch/paf-spsu/meetings/2007/M20-11/ min9.pdf; M. A. Furman, LARP CM12, Apr. 2009.

[5] M. Venturini et al., paper TUDP072 (these proceedings).

These results strengthen our tentative explanation, at least for extraction energy in a dipole bending magnet. For other cases, the results are less conclusive. In any case, the sensitivity of n_e on $E_{\max}$ is weak at nominal values of N_b, but may be significant at lower values of N_b.

The non-monotonicity of $n_e(N_b)$ has been noticed in earlier simulations for the SPS and the FNAL Main Injector upgrade [4], but not yet verified experimentally. We intend to further explore this phenomenon in the near future, via simulations and experiments at the SPS.

We have not yet methodically explored the sensitivity of our results to the details of the secondary electron emission spectrum. The above results assume a spectrum with a substantial rediffused component, which tends to yield higher
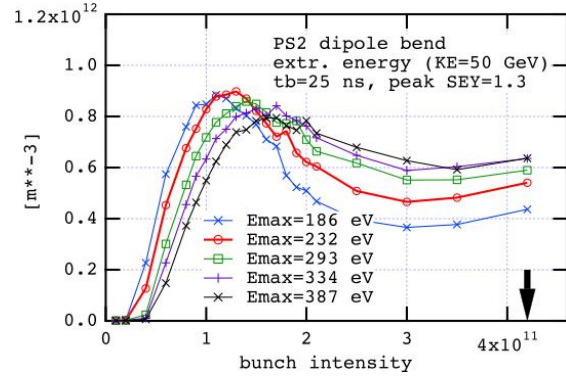
DISCLAIMER